

# FROM MEASUREMENT TO MODEL: ERS-1 SCATTEROMETER DATA ASSIMILATION

Ad Stoffelen  
European Centre for Medium range Weather Forecasts  
Reading, Berkshire, UK

## ABSTRACT

This paper will discuss the process of data characterisation before observations can be assimilated in numerical models. More specifically, we will discuss the most important characteristics of ERS-1 scatterometer data and its importance for Numerical Weather Prediction (NWP). We found that measurement noise is extremely low, and that uncertainties in the use of the data are merely a consequence of the interpretation of the measurements in terms of geophysical quantities on the spatial and temporal scale of the NWP model. We show that the measurements of radar backscatter,  $\sigma^0$ , can in good approximation be interpreted as observations of the 10 m surface wind vector. Collocation statistics of scatterometer retrieved winds show that these are more accurate than operationally available conventional surface wind observations. The low measurement noise makes it more practicable to use retrieved winds rather than  $\sigma^0$ 's as input for variational NWP data assimilation schemes. We will show the validity of this approach.

## 1. OBSERVATION SPACE

The scatterometer measures three values of normalised radar backscattered power,  $\sigma^0$ , from three different azimuth directions, at each node on the earth's surface. The triplet values may be represented as a three dimensional (3D) vector. We developed tools to visualise the 3D measurement space, and found that the  $\sigma^0$  triplets span a well-defined and cone-shaped surface [1, 2, 3, 4]. The opening of the cone is a measure of the anisotropy of the ocean surface backscatter, and related to wind direction retrieval skill. The extension of the cone in  $\sigma^0$  space is related to the amplitude of ocean capillary waves and consequently wind speed. The noise perpendicular to the surface, i.e.  $\sigma^0$  measurement noise, is low *Stoffelen et al* (1992), and would correspond to a typical deviation of a few tenth of a m/s in the components of the wind, given the sensitivity to wind. Specifically at low incidence angles, low wind speeds, and in cases of high temporal variability, the sensitivity of  $\sigma^0$  to other geophysical parameters such as wave conditions, slicks, SST, stability etc., may explain some of the  $\sigma^0$  variance perpendicular to the cone, not explained by instrumental noise. In preliminary tests, we didn't find any sensitivity of the cones position to SST and large-scale wave conditions. However, we observed increased noise close to (up to a range of 100-150 km) the centre of lows and fronts. It should be noted however, that a correlation of the  $\sigma^0$  variance perpendicular to the cone with one of these geophysical parameters would not have a significant impact on the perceived wind, because of the low noise. The cone consists of two leaves, one for when the system measures "upwind"

and one when measuring "downwind". Little difference in the location of these leaves is observed, resulting in a strong 180° ambiguity problem.

Provided we have an accurate mathematical description of the cone surface indicated by  $\mathcal{S}$ , then given a measured vector  $\sigma_o^0$ , we may be able to analyze the most probable value of the "true" vector  $\sigma_i^0$  lying on (or close to) the cone's surface. According to Bayes probability theorem we may write:

$$p(\sigma_s^0 | \sigma_o^0) = p(\sigma_o^0 | \sigma_s^0) \cdot p(\sigma_s^0) / p(\sigma_o^0)$$

where  $p(\sigma_s^0 | \sigma_o^0)$  is the conditional probability density for  $\sigma_s^0$  given a fixed  $\sigma_o^0$ . Equation (1) can be maximised for varying  $\sigma_s^0$ . The a priori probability density  $p(\sigma_s^0)$  is a constant in this process. The analysis equation requires a description of the a priori probability density of having a "true" triplet somewhere on the surface, i.e.  $p(\sigma_s^0)$ , where  $\sigma_s^0 \in \mathcal{S}$ . For convenience we may assume:

$$p(\sigma_s^0) = p(\sigma_{s1}^0 + \sigma_{s3}^0) \cdot p(\alpha)$$

Here  $\alpha$  is a cylindrical angular variable as depicted in Fig. 1. (The exact choice of the two parameters describing the surface is not significant at the moment, later on we will use wind speed and direction.)

Assuming  $p(\sigma_{s1}^0 + \sigma_{s3}^0)$  a constant, for  $|\sigma_s^0 - \sigma_o^0|$  close to or smaller than the measurement noise, will not have a significant impact on the retrieved  $\sigma_i^0$ , given the low measurement noise. Fig. 1a shows a cross-section through 3D measurement space, approximately in the plane of the angular variable  $\alpha$ . We can observe a distinct triangular shape. Given this geometry of the surface the probability of finding a certain number of  $\sigma^0$  triplets in an angular sector  $\Delta\alpha$ , depends on  $\alpha$ , and therefore  $p(\alpha)$  is not constant. Fig. 1b shows the same cross-section in 3D z-space after the transformation  $z_i = g(\sigma_i^0) = (\sigma_i^0)^{0.625}$ . Now the data lie on a conical surface  $\Sigma = g(\mathcal{S})$ , with an approximately uniform distribution in  $\alpha$ . Therefore, the assumption  $p(\alpha)$  is constant is appropriate in this space. We may assume that the conditional probability density  $p(z_o | z) = N(z, \epsilon)$ , where  $N$  is a 3D normal distribution with mean  $z$  and standard deviation  $\epsilon$ . Considering the distribution of triplets over the different cross-sections (not shown), this assumption of normal error distribution verifies to be adequate after the transformation.

Now we can formulate the *MLE* (Maximum Likelihood Estimator) as:

$$MLE = \frac{1}{|\epsilon(z_o)|^2} \sum_{i=1}^3 (z_{oi} - z_{si})^2$$

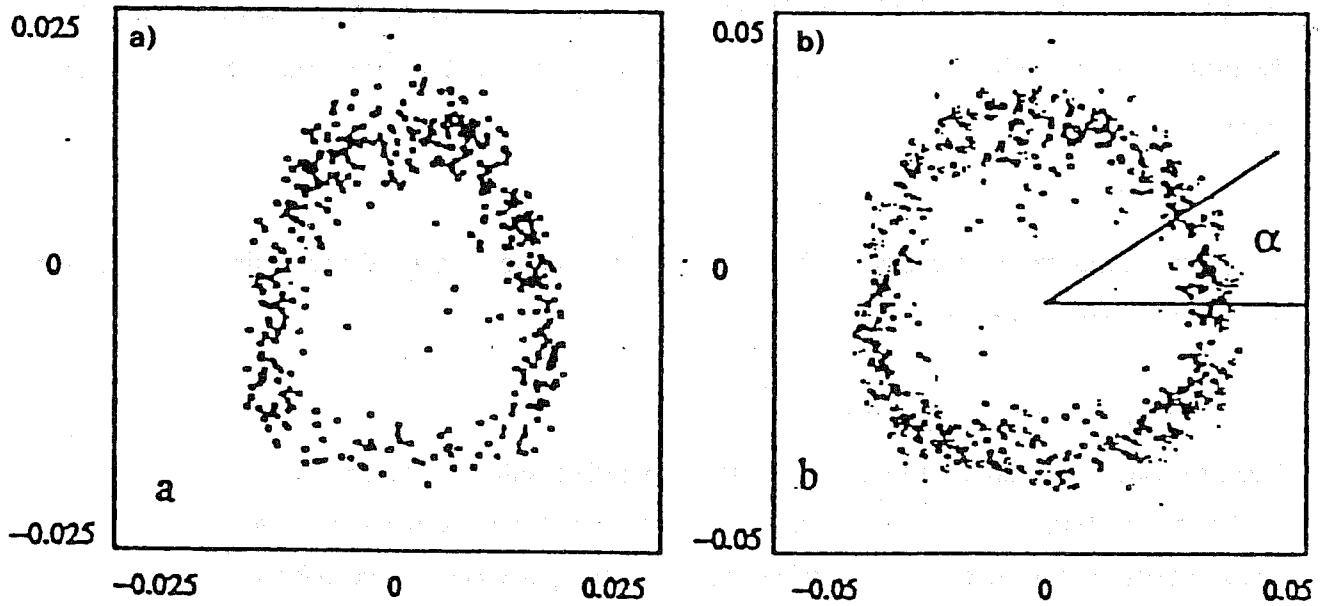


Fig. 1 Perpendicular cross-section through the cone surface of  $\sigma^0$ , (a), and  $z$ , (b), at a reference wind speed of  $\sim 8$  m/s, and for node 13 (from inside swath). The offsets for the centre of the plot are (0.017, 0.044, 0.019) (a) and (0.07, 0.12, 0.07) (b).

where the *MLE* has to be minimised with respect to  $z_{\Sigma} \in \Sigma$  in order to find the maximum probability estimate  $\sigma_r^0$  of  $\sigma_i^0$  *Stoffelen and Anderson (1993)*. Since the surface  $\Sigma$  (and  $S$ ) consists of two superimposed leaves, in general two solutions exist. The term involving  $\epsilon$  is such that for the solution  $\langle MLE \rangle = 1$ , i.e. the expected value for the residual is unity. When the description of the surface, can not be assumed to be perfectly accurate, i.e. has accuracy  $\epsilon_s$ , then in the above calculations  $\epsilon$  should be replaced by:

$$\epsilon_T = (\epsilon_s^2 + \epsilon^2)^{1/2}$$

So, given a measured  $\sigma^0$  triplet(s) we have derived a method to compute the most likely corresponding triplet on the cone's surface.

## 2. QUALITY OF RETRIEVED WINDS

The next step is to assign a geophysical meaning to each position on the cone's surface. In general, a surface can be described by two parameters. Our first aim is to retrieve wind speed and direction from the scatterometer measurements, and therefore we use these parameters to describe the surface. Using adequately filtered data sets of collocated  $\sigma^0$ 's and ECMWF analysis 10 m wind vectors, we ran a *MLE* procedure to determine the parameters of an empirically formulated  $\sigma^0$ -to-wind transfer function [2]. Naturally, the first diagnostic of a newly derived transfer function is its ability to describe the cone's surface within the proportions of measurement noise. In general, *CMOD4 Stoffelen and Anderson (1992)* fits the cone's surface within measurement noise, and consequently the *MLE* as computed from equations (3) and (4) has an average value of 1.4, when  $\epsilon_s$  is assumed zero. This verifies the good fit of *CMOD4* to the cone's surface, and the validity of our  $\sigma^0$  noise estimates.

The second diagnostic is to verify retrieved winds computed from the transfer function and the retrieval scheme as described in previous section. ESA's ERS-1 analysis team compared several proposals for transfer functions from groups throughout Europe and a proposal from Freilich, on the basis of wind verification *Offiler (1992)*. On its recommendation ESA has implemented the ECMWF transfer functions (*CMOD3*, and later *CMOD4*) in daily operations. Not surprisingly, we found a strong correlation in the ability of a transfer function to fit the cone's surface and its potential for wind retrieval.

Since measurement noise is low, the main uncertainty in wind retrieval will be the sum of transfer function error and representativeness error. These errors account respectively for geophysical dependencies, other than wind, not taken into account in the transfer function, and for the mismatch in spatial and temporal scales between the observations and the NWP model. In Fig. 2 we show 2D histograms of collocations of

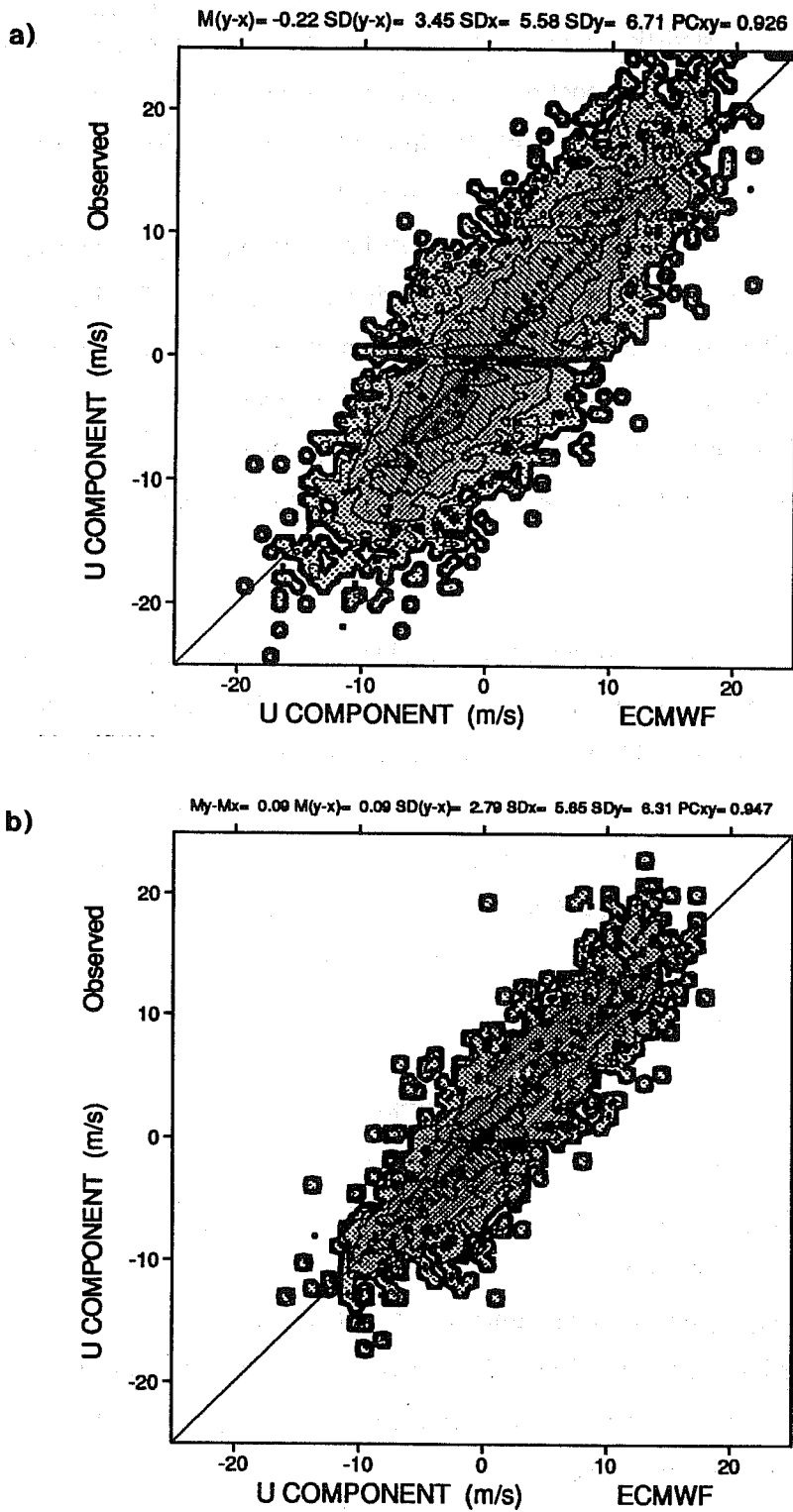


Fig.2 Collocation histogram of the East-West component of the wind for ECMWF guess field winds (FGAT) and non-automatic SHIP (a) and automatic SHIP, as received on GTS. Observations with a direction departure of more than  $90^\circ$  are rejected. For (a) the standard deviation of the departure is 3.45 m/s, the correlation 0.93, and the wind speed bias 1.41 m/s, for (b) these figures are respectively 2.79 m/s, 0.95 and 0.73 m/s.

automatic (2a) and non-automatic (2b) SHIP winds and NWP forecast winds for the East-West component of the wind. These departure statistics incorporate all contributions to the observation error such as discussed above, but also the ECMWF model error including an error due to the extrapolation from the lowest model level to 10 m height. A difference of 10% in wind speed bias exists between non-automatic, and automatic ship. Further, the lower quality of non-automatic SHIP is evident. We made similar statistics for other data sets operationally available on GTS, i.e. moored and drifting buoys, and automatic and non-automatic island stations, which again are mutually not consistent. The reason for this may lie in several facts, such as different distributions of the observational data across the globe, a difference of quality in the observational systems, and no or insufficient height correction (WMO requires a measurement to be reported at 10 m height). CMOD4 was derived from ECMWF model winds, and therefore biases in the model need to be corrected. The above inconsistencies make it very difficult to decide upon a correct scaling of the wind speed strength.

Similar to Fig 2, we show in Fig 3 2D histograms of collocations of retrieved scatterometer winds and NWP forecast winds for node 11 across the swath. For the wind component collocation plots of scatterometer data we computed the highest correlation with the NWP model (97%), amongst all the other conventional data sets. This indicates that the scatterometer winds are more accurate than any other operationally available surface wind data set. The departure statistics for wind speed and direction, and for the components of the winds were mutually consistent for all comparisons we made. For a few nodes at the inner swath, we noted an increased measurement noise [4], which results in a slightly decreased wind component correlation (95%), but still comparable to the conventional data sets.

Table 1 shows departure statistics of scatterometer minus ECMWF forecast winds, separately for wind speed and direction, and for each odd across-swath node. The error, due to the smaller scale of representativeness of scatterometer data (50 km), compared to the NWP model (~120 km), may be estimated to be ~1 m/s in the components of the wind, and should not vary with node number. The ECMWF contribution should also be the same for all cells, and given the node-to-node variation in statistics we may conclude that the scatterometer error contribution must be significant for at least some nodes. If we assume for instance, that the partitioning between model error and scatterometer observation error is equal for cell 11, we could characterize the scatterometer error for all cells.

From table 1 we can see that the departure standard deviation for wind speed increases with increasing node number, whereas for wind direction it decreases. We may also note that in the inversion with CMOD4 a small wind speed bias appears, the nature of which should be investigated and if necessary corrected for. The departure vector RMS decreases with increasing node number, indicating that the overall error of the scatterometer winds is lowest at high incidence angles. The future ESA Advanced scatterometer system

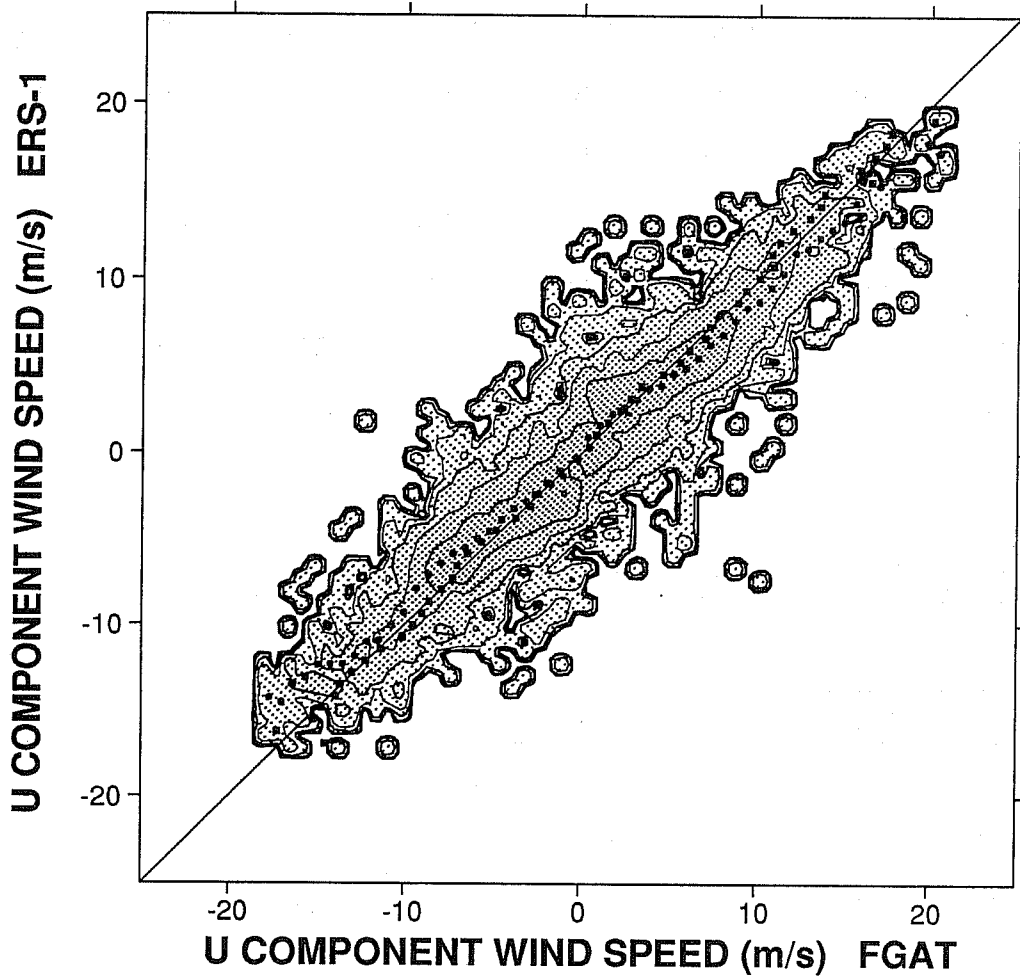


Fig.3 Collocation histogram of the component of the wind in the direction of the mid beam for node 11 (from inside swath) for ECMWF guess field winds (FGAT) and ERS-1. The closest of two available ERS-1 solutions to the short-term forecast, is selected. The standard deviation of the departure is 2.20 m/s, the correlation 0.97, and the wind speed bias -0.2 m/s.

Cell	Nbr.	Bias	Sd	Vrms	Nbr.	Bias	Sd	Vrms
1	9168	0.88	23.81	3.73	10883	-0.48	1.93	3.54
3	9511	0.92	21.13	3.37	11008	-0.41	1.94	3.24
5	9717	1.26	19.89	3.21	11199	-0.30	1.96	3.10
7	9783	1.46	19.17	3.16	11355	-0.28	1.97	3.05
9	9794	1.10	19.07	3.17	11472	-0.26	1.99	3.05
11	9762	1.42	18.86	3.15	11480	-0.24	1.98	3.02
13	9700	1.48	18.69	3.15	11526	-0.25	2.00	3.01
15	9656	1.29	18.71	3.15	11545	-0.25	2.05	3.02
17	9638	1.11	18.31	3.14	11564	-0.24	2.07	3.00
19	9677	0.98	18.36	3.11	11616	-0.24	2.04	2.98

Table 1 Departure statistics of ERS-1 minus ECMWF analysis wind speeds (right) and directions (left), for all odd nodes (numbered from inside swath). Direction statistics are only made when the average wind speed exceeds 4 m/s.

Cell	Nbr.	Bias	Sd	Vrms	Nbr.	Bias	Sd	Vrms
1	10128	-0.06	8.22	1.29	12317	-0.01	0.60	1.12
3	10032	0.10	5.89	0.95	12205	-0.01	0.47	0.89
5	10082	-0.01	4.92	0.79	12372	0.00	0.40	0.74
7	10139	0.10	3.37	0.57	12585	-0.01	0.30	0.54
9	10101	0.00	3.09	0.53	12597	-0.01	0.28	0.49
11	10085	-0.03	2.83	0.50	12590	-0.01	0.27	0.46
13	10045	0.00	2.69	0.47	12604	-0.01	0.26	0.44
15	9921	-0.01	2.54	0.45	12579	-0.01	0.24	0.42
17	9830	0.03	2.47	0.45	12478	-0.01	0.24	0.42
19	9878	-0.02	2.39	0.44	12505	0.01	0.24	0.41

Table 2 As Table 1, except for retrieved winds from simulated  $\sigma^0$ 's. The ECMWF analysis  $\sigma^0$ 's were distorted by our estimate of measurement noise [2].



(ASCATT) will therefore have its swath moved to higher incidence angles. It is clear that the sensitivity of the scatterometer to the wind vector is the main effect. Other geophysical parameters should however be investigated for correlation with the remaining departure errors.

Table 2 is similar to Table 1, but here the scatterometer winds are computed from simulated  $\sigma^0$ 's. The simulation is done by computing  $\sigma^0$ 's from the ECMWF analysis winds using CMOD4, and consequently disturbing those by the measurement noise, as explained in the previous section. Indeed, we observe that measurement noise is very low, and only accounts for an insignificant contribution to the total scatterometer wind error.

Global departure statistics provide a good general characterisation of observation measurement error, but fail to give a complete picture of the usefulness of data. For scatterometer data, we investigated numerous interesting and complicated cases in order gain experience in how to deal with the data. Especially ambiguity removal is a difficult task (see next section). Fig 4 shows a typical example of such a case. The scatterometer data in Fig 4a contain considerably more detail than the ECMWF short range forecast in Fig 4b, a statement that is generally valid. Therefore we expect that the horizontal correlation of scatterometer wind error is not significant, and that these wind errors have a random, rather than a systematic nature.

### 3. DATA ASSIMILATION

Given the accuracy of the retrieved scatterometer winds, it certainly seems worthwhile to assimilate the data into NWP models. At the ECMWF statistical interpolation (OI), and 3D and 4D (time coordinate added) variational methods (resp. 3D-VAR and 4D-VAR) are in use for meteorological analysis.

### 4. OI

The OI analysis is a linear combination of the observations and a meteorological short-range forecast, or guess. All information is weighted according to its estimated accuracy, and is distributed according to estimated covariances between different meteorological parameters at different locations. In order to use scatterometer data in this scheme, the winds have to be made unambiguous.

At ECMWF we developed an ambiguity removal scheme, that is initialised by the solution closest to the guess field. The initial confidence in the solution is determined by a parameter called wind direction retrieval skill derived from the position of a measured  $\sigma^0$  triplet relative to the cone, the vector difference between the scatterometer solution and the guess, the number of neighbours, and the number of solutions (which is 2 in ~ 95% of the cases). The horizontal vector filter operates on a grid of 5 by 5 nodes at a

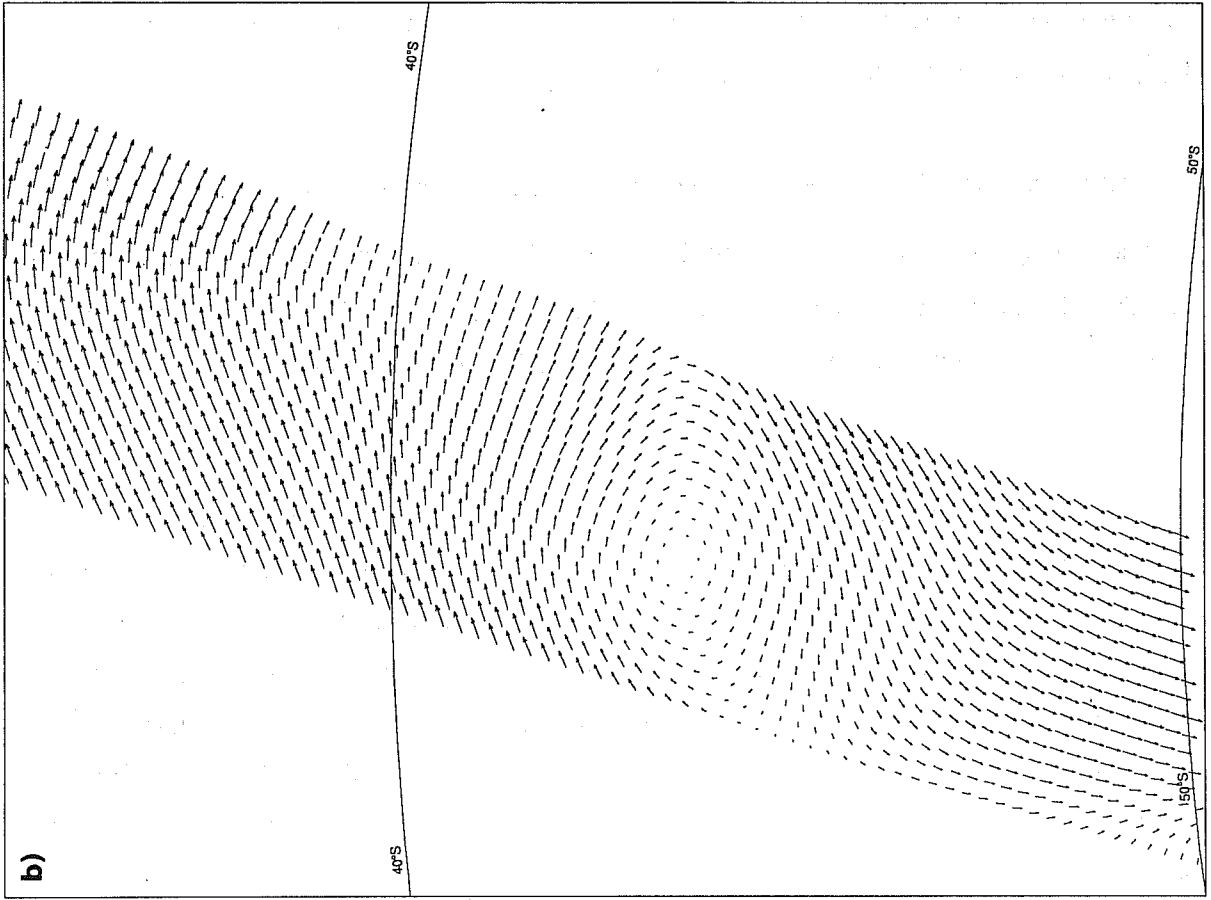
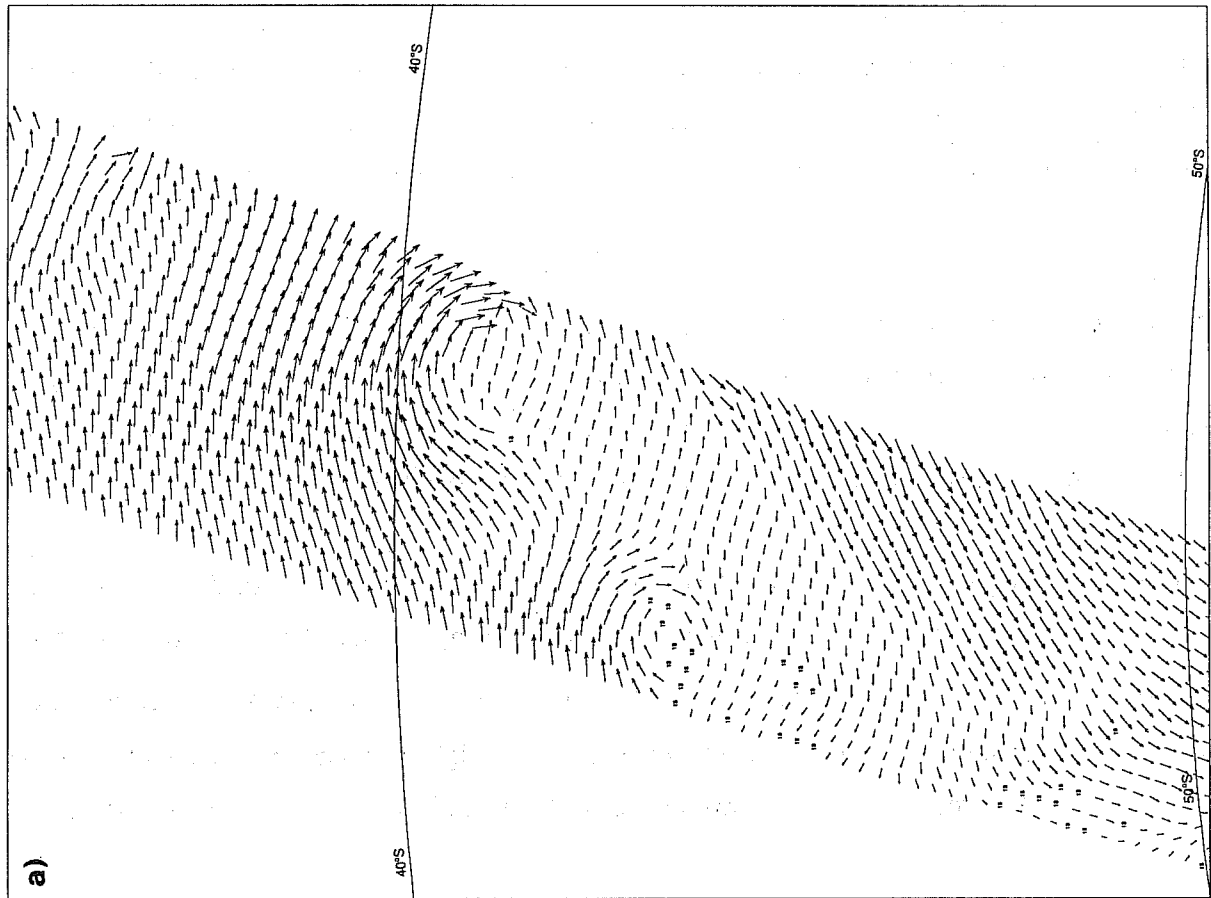


Fig.4 Solutions of the ECMWF PRESCAT ambiguity removal for ERS-1 data around 170W and 40S on 99/03/26 00GMT (a), and the corresponding ECMWF guess field (PRESCAT) used in the processing (b).

time, and updates the scatterometer solution in the centre of the grid, if the average weighted vector difference of the solution with its neighbours is smaller than for the current solution. The magnitude of this average weighted vector difference determines the amount by which the confidence in the solution is increased. We found that this scheme is very efficient in adjusting phase errors present in the guess field (e.g. as in Fig 4). The OI performs a check, called "buddy" check, where it compares an observation with an analysis comprising all observations except the one being checked. The buddy check is used effectively in removing, rarely occurring, small areas of erroneous vectors (~0.1% of cases). Thus, the current ambiguity removal/OI scheme works satisfactory.

Analysis and forecast experiments carried out using the above described wind product show positive analysis and short term forecast impacts. More specifically, we found that a 12 hour forecast run from an analysis using scatterometer data fits scatterometer data significantly (~ 5%) better, than a forecast run from an analysis without scatterometer data. Also, for upper air data the 6 hour forecast is improved, when scatterometer winds are used in the analysis. We further identified cases where the ambiguity removal is improved when scatterometer data has been used in previous analysis. 5-day forecasts show a neutral impact with respect to the winds. However, a significant positive impact is found when NOAA TOVS are not used in the analysis, suggesting a redundancy for medium range forecasting (i.e. on larger synoptic scales) of scatterometer winds and NOAA TOVS.

## 5. VARIATIONAL METHODS

In a variational data assimilation scheme linearised equations around the solution state are used in a minimisation in order to solve a non-linear analysis problem. An implicit ambiguity removal for scatterometer data would be helped by meteorological balance constraints on differences between the control variables and the guess field, incorporated in the penalty term  $J_b$ . Recent studies show that in a 4D-VAR system baroclinic structures can be enforced by assimilating surface (i.e. scatterometer) data *Thépaut et al* (1992).

In the variational approach a cost function  $J$  is introduced:

$$J = J_o + J_b$$

where  $J_o$  is the penalty term associated with the difference between the control variables and the observations. Following *Lorenc* (1986), we may specify the contribution of scatterometer data to this cost function as:

$$J_o^{SCAT} = -2 \ln[ p(\sigma_o^0 | V) ]$$

where  $V$  is the estimate for the local wind vector. Further:

$$p(\sigma_o^0|V) = \int_{\sigma_s^0} p(\sigma_o^0|\sigma^0) p(\sigma^0|V) d\sigma^0$$

The integral is over  $\sigma_s^0$ , i.e. the cone surface as described by the transfer function. The first term in the integral should express  $\epsilon_T$  as formulated in equation (3), i.e. the noise observed perpendicular to the cone's surface, which we discussed earlier. The second term should express our knowledge about the errors made when interpreting  $\sigma_s^0$  as the "true" wind vector and about the retrieved wind vector's misrepresentation of the NWP model spatial and temporal scales. One could attempt to assimilate  $\sigma_o^0$  directly in our NWP model, and project the transfer function and representativeness error, which have their only contribution along the surface  $S$  and are therefore well characterised by the wind parameters, onto  $\sigma_s^0$ . Because the  $\sigma^0$  to wind relationship as represented by the curved cone surface is highly non-linear, the projection of wind errors onto the cone is a complex problem. Certainly plane approximations using only  $\partial\sigma_s^0/\partial V$  will be inappropriate. Using the curvature, i.e.  $\partial^2\sigma_s^0/\partial V^2$  should of course be better, although still not perfect, and will certainly result in an algorithm of substantial mathematical complexity and computational cost. Moreover, in an attempt to strive for mathematical elegance, one would forget that the uncertainties in our knowledge of  $\partial^2\sigma_s^0/\partial V^2$  may be of a limiting adequacy.

Alternatively, one could try to formulate the problem in terms of wind. For this purpose, we will have to make some approximations concerning equation (7). As discussed in (Ref. 1), we can accurately identify the most likely "true" position of a measured  $\sigma^0$  triplet on the cone's surface, and we have shown in Table 2 of this paper the uncertainties it introduces in the wind domain. When comparing to Table 1, we argued measurement noise is that low, it may be neglected. Therefore, replacing  $p(\sigma_o^0|\sigma_s^0)$  by  $p(\sigma_r^0|\sigma_s^0)$ , with  $\sigma_r^0$  as derived from the retrieval (Ref. 1) is a valid approximation. The retrieval has multiple solutions  $\sigma_r^{oi}$  because of the 180° ambiguity, and therefore the first term in the integral will be a sum of  $p(\sigma_r^{oi}|\sigma_s^0)/n$  with  $i = 1, \dots, n$  the solution index. Here, we have assumed no skill in the distinction of the different  $\sigma_r^{oi}$ , i.e. all solutions have probability  $1/n$ . Although in our retrieval, we have ~ 5% of cases with more than two acceptable solutions, we find that all the solutions in these cases are of dubious quality, and limiting ourselves to two of the solutions has no impact on the departure statistics and the quality of the retrieved wind fields. Therefore, we take  $n = 2$ .

When we assume isotropic  $\sigma^0$  measurement errors in 3D  $\sigma^0$  space, then a further replacement of  $p(\sigma_r^{\text{alt}}|\sigma_s^0)$  with a Kronecker  $\delta$ -function of the form  $\delta(\sigma_r^{\text{alt}} - \sigma_s^0)$  is an equally valid assumption compared to the first one. Now, after integration and using the transfer function to map  $\sigma_r^{\text{alt}}$  onto the retrieved winds  $V_r^i$ , equation (7) reduces to  $p(\sigma_o^0|V) = p(V_r^1|V)/2 + p(V_r^2|V)/2$ . In this case, the formulation of the problem in wind space only needs a proper characterization of the sum of transfer function error and the representativeness error in wind space, as was being achieved in the first paper (Ref 1). We may assume  $p(V_a|V) = p(V|V_a) = N(V_a, \epsilon_r)$  for an unambiguous scatterometer wind  $V_a$ , i.e. normal distributed around the components of  $V$  with error  $\epsilon_r$ . Similarly, for the ambiguous solutions we may write  $p(\sigma_o^0|V) = N(V_r^1, \epsilon_r)/2 + N(V_r^2, \epsilon_r)/2$ . From equation (6) we derive the scatterometer cost function, which will not be quadratic particularly when  $\|V - V_r^1\| = \|V - V_r^2\| \leq |\epsilon_r|$ . Moreover, in these cases we find only one minimum at  $V = 0$ .

An alternative analytic formulation can be found, that describes a conditional functionality in terms of the penalty function  $J_o^{\text{SCAT}}$ :

$$J_o^{\text{SCAT}} = \left( \frac{\prod_i K_i}{\sum_i K_i} \right)^{\frac{1}{P}}$$

with  $K_i = \{J_{\alpha}^S(V_r^i)\}^P$ , and e.g.  $P = 4$ .  $J_{\alpha}^S$  characterises the estimated scatterometer wind error for one single solution, and is assumed quadratic as before. This  $J_o^{\text{SCAT}}$  cost function has also for low speeds two minima exactly located at  $V_r^1$  and  $V_r^2$ , and almost in the entire speed domain a quadratic dependency on  $V$ , except where  $V - V_r^1 = V - V_r^2$ . Therefore, this formulation has more symmetry around its minima. For  $P < 4$  we have a weaker gradient towards the minima, or in other words, exact ambiguity removal will be less of a constraint and intermediate solutions more likely. However, from our experience with ambiguity removal we believe that a strong constraint is more appropriate, but this needs to be tested.

To investigate the statistical consequence of the cost function formulation, we performed Monte Carlo simulations.  $V_r^1$  and  $V_r^2 = -V_r^1$ , and a background wind  $V_b$  were simulated for a given  $V$ , using respectively a Gaussian wind component error of  $\epsilon_r$  and  $\epsilon_b$  for the scatterometer and background wind (in

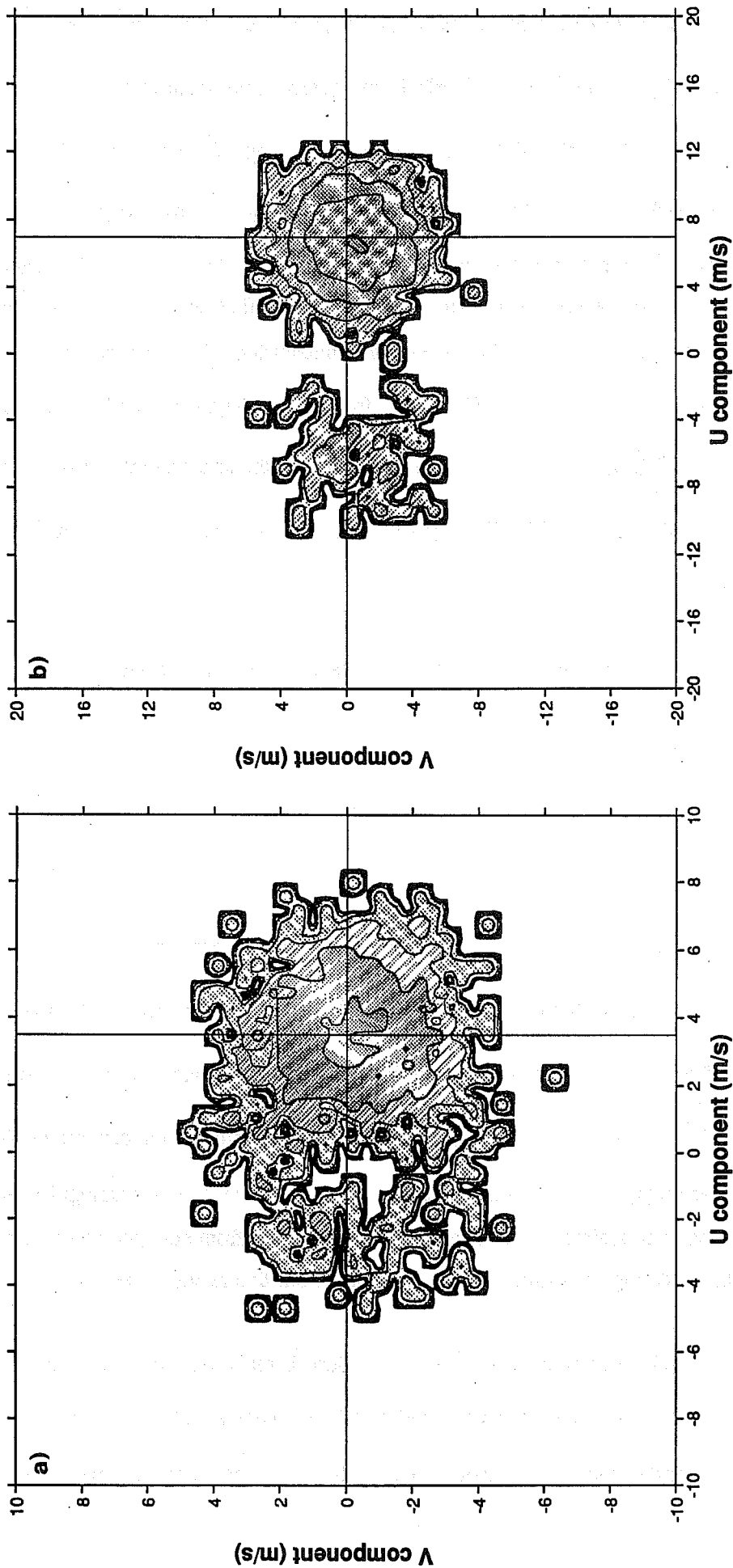


Fig.5 Monte Carlo simulations as explained in the text, with a true wind speed  $V = (3.5, 0)$ , and noise  $\epsilon_r = 2$  m/s and  $\epsilon_b = 2$  m/s. The solution points are calculated with  $J_0^{scat} = J_0^S J_{\sigma_0}^S [J_{\sigma_0}^S + J_{\sigma_0}^S]^{1/2}$ . The mean retrieved U-component is 3.25 m/s (a). (b) is for  $V = (7, 0)$ , and noise  $\epsilon_b = 4$  m/s. The mean retrieved U is 6.44 m/s with standard deviations of 3.29 m/s for U and 1.84 m/s for the V component. 2000 simulated scatterometer and background winds are used for (a) and (b).

fact  $\epsilon_b$  characterises the accuracy of all available information, except the observation under investigation). Fig 5a shows a result when minimising equation (5) with the above scatterometer cost function for 2000 trials. We can observe that ambiguity removal is generally successful for a speed as low as 3.5 m/s. Fig 5b shows, similarly to 5a, the distribution of solutions for 2000 simulations, but in this case for  $\epsilon_b = 4$  m/s and  $V = 7$  m/s. As expected, it can be seen that ambiguity removal is less successful with reduced supporting wind direction information. The statistical difference between the two proposed cost functions is marginal, and therefore, because of the more symmetric and quadratic behaviour, the functionality in equation (8) may be more desirable. With equation (8), we have arrived at a practicable and accurate solution for the variational assimilation of scatterometer observations. At ECMWF we are currently developing an algorithm along these lines.

## 6. SUMMARY

Considering the characteristics of 3D  $\sigma^0$  measurement space we found an optimal procedure to derive the most likely "true"  $\sigma^0$  on the well-defined solution surface. The uncertainty in the wind speed and direction which it represents can easily be characterised in the wind domain, and we find that scatterometer wind retrievals are in general more accurate than conventional surface wind measurements. Clearly, the first order deliverable of scatterometer radar measurements is the wind vector, and additional geophysical parameters may only have small, but possibly beneficial impact on the wind product. The 180° ambiguity of the winds poses a difficult problem for data assimilation. Starting from existing ambiguity removal schemes we developed at ECMWF a new algorithm, that proves to work satisfactorily in combination with the OI data assimilation scheme. Variational assimilation of scatterometer winds, rather than  $\sigma^0$ 's, seems the most straightforward and practicable way forward. Ambiguity removal skill is expected to be higher in a variational data assimilation scheme, but this statement needs verification in the coming years. By comparison to conventional observations, cloud drift winds, cloud imagery, and ECMWF analysis and forecasts we found that the scatterometer winds possess significant synoptic detail, which proves potentially useful for NWP and climate studies.

## ACKNOWLEDGEMENTS

I would like to acknowledge ECMWF staff, and in particular Dave Anderson, Catherine Gaffard, John Eyre, and Philippe Courtier for useful discussions contributing to this paper. ECMWF and ESA resources were gratefully accepted to carry out the work.

## REFERENCES

A C Lorenc, 1986: "Analysis methods for numerical weather prediction", Q J R Meteorol Soc, 112, pp 1177-1194.

D Offler, 1992: "CMOD Model Tuning (Phase III)", report for the ERS-1 analysis team meeting, Frascati, Italy, 9 November.

A C M Stoffelen and D L T Anderson, 1992: "ERS-1 scatterometer calibration and validation activities at ECMWF: A. The quality and characteristics of the radar backscatter measurements", in Proc. European 'Int. Space Year' Conf., Munich, Germany, 30 March - 4 April.

A C M Stoffelen, D L T Anderson, and P M Woiceshyn, 1992: "ERS-1 scatterometer calibration and validation activities at ECMWF: B. From radar backscatter characteristics to wind vector solutions", referenced as above.

A Stoffelen, and D L T Anderson, 1992: "ERS-1 scatterometer data characteristics and wind retrieval skill", presented at the First ERS-1 Workshop, Cannes, France, 4-6 November.

A Stoffelen and D L T Anderson, 1993: "Wind retrieval and ERS-1 radar backscatter measurements", Adv. Space Res. Vol. 13, No. 5, pp. (5)53-(5)60.

J-N Thépaut, P Courtier, R N Hoffman, 1992: "Use of dynamical information in a 4D variational assimilation", presented at the ECMWF workshop on variational assimilation with emphasis on 3 dimensional aspects, Reading, UK, 9-12 November.